Optics Letters

Combined multi-band infrared camouflage and thermal management via a simple multilayer structure design

Lei Wang,[1,†] Yue Yang,[2,*,†] Xianglin Tang,[1] Bin Li,[1] Yizhi Hu,[1] Yonggang Zhu,[2] and Huizhu Yang[2]

[1]School of Science, Harbin Institute of Technology, Shenzhen 518055, China
[2]School of Mechanical Engineering and Automation, Harbin Institute of Technology, Shenzhen 518055, China
*Corresponding author: yangyue2017@hit.edu.cn

Received 30 August 2021; revised 17 September 2021; accepted 21 September 2021; posted 28 September 2021 (Doc. ID 441605); published 15 October 2021

Infrared camouflage is crucial for high-temperature objects to avoid detection, and spontaneous infrared radiation is also an important way for high-temperature objects to dissipate heat. Therefore, selective infrared emission has become significant for the coating design of surfaces such as aircraft, which require low emission in the atmospheric window band (3–5 μm and 8–14 μm) and high emission outside it (5–8 μm). This Letter employs a simple multilayer film structure to achieve selective regulation of the material emission spectrum. Combining the transfer matrix method and genetic algorithm, a multilayer film structure containing 12 layers of three high-temperature-resistant materials (SiO_2, TiO_2 and Ge) has been designed. It shows fairly low emissivity in two main bands of infrared detection ($\varepsilon_{3\sim5\ \mu m} = 0.14$, $\varepsilon_{8\sim14\ \mu m} = 0.21$) and high emissivity outside them ($\varepsilon_{5\sim8\ \mu m} = 0.86$), and this infrared selectivity can be well maintained with the incident angle rising from 0 to 60 deg. The Poynting vector distribution in the material at different incident wavelengths is analyzed to further explore the interference mechanism to achieve spectral selective emission. The significance of this work lies in the construction of a relatively simple coating design while ensuring efficient infrared camouflage and thermal management performance.

https://doi.org/10.1364/OL.441605

With the continuous development of infrared detection technology and electronic information processing systems, many infrared technologies (such as infrared detection, infrared night vision, and infrared guidance) have become increasingly popular in the military field [1]. The main working bands of infrared detection are 3–5 μm and 8–14 μm, corresponding to the two atmospheric window bands where the ambience does not absorb the signal [2–5]. By reducing the emissivity of the object surface at the atmospheric window bands, it can effectively avoid infrared detection to achieve infrared camouflage [6–8]. In previous studies to achieve infrared camouflage, scholars mostly used surface coating materials with lower emission throughout the whole mid-infrared band. Those surface coating materials mainly include structures of metasurfaces [4,9], insulated metal nanowires [10], core–shell composites [11–13], and thin films (such as metals [14] and semiconductors [15,16]). Since spontaneous radiation is an important heat dissipation mechanism method for high-temperature surfaces, the suppression of thermal emission can lead to overheating. Therefore, researchers proposed the strategy to achieve selective emission in the mid-infrared range to fulfill the requirements of both infrared camouflage and thermal management, i.e., designing a coating material with low emission at the infrared detection spectrum (3–5 μm and 8–14 μm) and high emission outside it for heat dissipation purpose [7,17,18].

The types of structures applied to achieve selective emission in the infrared range mainly focus on camouflage photonic crystals [19–23], resonant metamaterial [24,25], and multilayer films [26–28]. Recently, Pan *et al.* [28] prepared a three-layer thin film composed of Si, $Ge_2Sb_2Te_5$ and Au, which could achieve a low emissivity of 0.17 and 0.13 in the 3–5 μm and 8–14 μm bands, respectively, and a high emissivity of 0.77 in the 5–8 μm band. Peng *et al.* [26] also designed a Ag/Ge multilayer film based selective emitter for infrared camouflage using an ultrathin metal film and impedance matching to tune the radiation characteristics. The prepared film demonstrated good spectral selectivity in the infrared range with a low emissivity in the atmospheric window ($\varepsilon_{3\sim5\ \mu m} = 0.18$, $\varepsilon_{8\sim14\ \mu m} = 0.31$), and a high one outside it ($\varepsilon_{5\sim8\ \mu m} = 0.82$). Compared to periodic photonic crystal and resonant metamaterial structures, multilayer films are easier to fabricate. Although existing studies have already demonstrated good spectral selectivity with a multilayer film, most of them contain metal films, which are not stable at a high temperature and would deteriorate their performance. In addition, there is still room to improve the performance of selective infrared emitters with lower emission in the detection band and higher outside it.

Considering the easy-to-fabricate and relatively better spectral selectivity characteristics of multilayer film structures, we select three commonly used high-temperature endurable materials of SiO_2, TiO_2 and Ge [22,23] to compose a coating

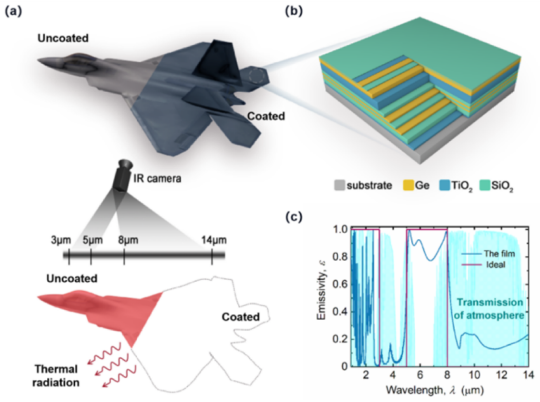

Fig. 1. (a) Schematic diagram of the film covering the aircraft surface to achieve multi-band infrared camouflage and heat dissipation management functions at the same time. (b) Schematic diagram of the multilayer film structure formed by alternate deposition of SiO_2, TiO_2 and Ge. (c) Infrared emissivity spectra of the designed film and ideal surface.

on the substrate of SiO_2 and design a selective infrared emitter in the present study for purposes of both infrared camouflage and heat dissipation. The refractive indices and extinctions of these three materials are discussed in Supplement 1. The properties are plotted in Fig. S2. The large refractive index contrast and differences in absorption regions are the basis for strong interference and selective absorption. Combining the transfer matrix method and a genetic algorithm, a 12-layer film structure has been designed, and shows fairly low emissivity in two main bands of infrared detection ($\varepsilon_{3\sim5\ \mu m} = 0.18$, $\varepsilon_{8\sim14\ \mu m} = 0.31$) and high emissivity outside them ($\varepsilon_{5\sim8\ \mu m} = 0.82$). This work can provide significant guidance for the design of infrared camouflage coatings with thermal management.

As shown in the schematic diagram of Fig. 1(a), the function of the selective infrared emitter designed in this study is to realize multi-band infrared camouflage and heat dissipation through thermal radiation at the same time. Taking the aircraft surface covered with the coating as an example, infrared detection can be avoided by reducing the emissivity within the atmospheric window spectrum (i.e., 3–5 μm and 8–14 μm). On the other hand, increasing the emissivity outside the atmospheric window (i.e., 5–8 μm) is beneficial for heat dissipation to cool the surface, which can avoid thermal instability and weaken the thermal emission at the detection spectrum as well by decreasing the surface temperature.

Figure 1(b) shows a schematic of the thin-film coating structure designed in this study, which is a multilayer thin-film structure formed by alternately depositing 12 layers of SiO_2, TiO_2 and Ge. The infrared emissivity spectrum of the proposed multilayer film is shown in Fig. 1(c). The infrared emissivity spectrum of an ideal surface is also shown in Fig. 1(c) for comparison. Considering that the aircraft surface temperature may vary in a large range, as from 300 K to 1000 K considered in this study, the emissive energy would blueshift to the near-infrared band, so we also set the ideal emissivity at the wavelength range of 0.3–3 μm as unity, which considers only the effect of self-emission and does not include the absorption from solar radiation. The proposed thin film achieves an infrared selective emission close to the ideal one. The spectral emissivity among the whole spectrum range of 3–5 μm is below 0.15, and that for

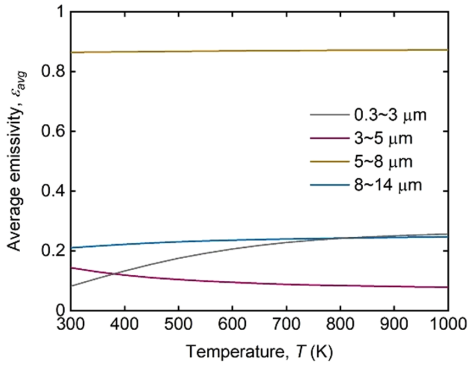

Fig. 2. Average emissivity of proposed film for each spectrum range of 0.3–3 μm, 3–5 μm, 5–8 μm, and 8–14 μm as a function of its temperature.

8–14 μm is below 0.25, while that for the 5–8 μm spectrum is always above 0.8. There is a sharp change of spectral emissivity at the boundary of 5 μm and 8 μm. Based on the spectral infrared emissivity presented in Fig. 1(c), we further calculated the average emissivity for each spectrum range under different temperature conditions, which is more straightforward to quantify the performance of the proposed film for both infrared camouflage and heat dissipation. The average emissivity ε_{avg} of the material between wavelengths of λ_1 and λ_2 can be obtained by the following formula:

$$\varepsilon[\lambda_1, \lambda_2]_{avg} = \int_{\lambda_1}^{\lambda_2} \varepsilon(\lambda) I_{BB}(\lambda, T)\mathrm{d}\lambda \Big/ \int_{\lambda_1}^{\lambda_2} I_{BB}(\lambda, T)\mathrm{d}\lambda. \quad (1)$$

Here $I_{BB}(\lambda, T) = 2hc^2/\lambda^5 \cdot [\exp(hc/\lambda k_B T) - 1]^{-1}$ is the radiated energy of a blackbody at a wavelength of λ and temperature of T according to Planck's law. $\varepsilon(\lambda)$ is the spectral emissivity of the film in the normal direction.

Figure 2 shows the average emissivities for the four ranges as a function of temperature. The average emissivities in the 3–5 μm and 8–14 μm spectrum ranges display a slight decrease from 0.14 and increase from 0.21, respectively, as the temperature rises, while the emissivity in the 5–8 μm band always remains at about 0.86. This is because the peak of the object's radiant energy will blueshift to a short wavelength as the temperature increases, and the average emissivity may decrease, increase, or not change according to the spectral emissivity distribution in each spectrum range. The reason for the low emissivity around 0.2 in the 0.3–3 μm spectrum range is due to the near-zero emissivity between 2.5 μm and 3 μm, and there is a sharp decrease in radiative energy below 2.5 μm even at a high temperature. To sum, the proposed film maintains a fairly good performance for both infrared camouflage, with average emissivity below 0.2, and heat dissipation, with average emissivity above 0.85 in the mid-infrared range, as the temperatures rises from 300 K to 1000 K.

We have also employed a genetic algorithm [29] to help realize multi-parameter optimization, including the selection of layer number, thickness, and material, to achieve an emission spectrum closest to the ideal. Figure 3(a) gives the objective function of optimization, which is consistent with the ideal emission spectra shown in Fig. 1. Figure 3(b) presents the detailed workflow of the optimization process with the genetic algorithm and under the framework of transfer matrix theory

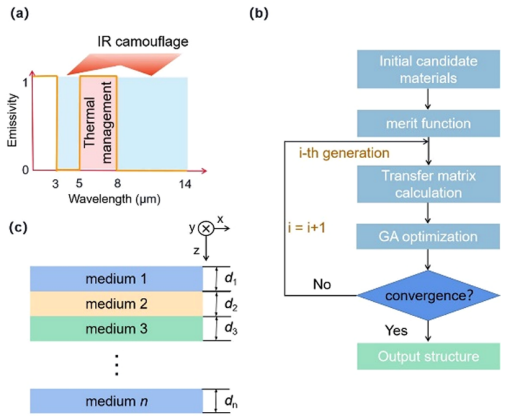

Fig. 3. Process of the multilayer film design. (a) The ideal selective infrared emission with an emissivity of zero at 3–5 μm and 8–14 μm spectrum range and an emissivity of one outside is considered as the objective function of optimization. (b) Flow chart to obtain optimized film structure with genetic algorithm; (c) schematic diagram of the desired multilayer film structure.

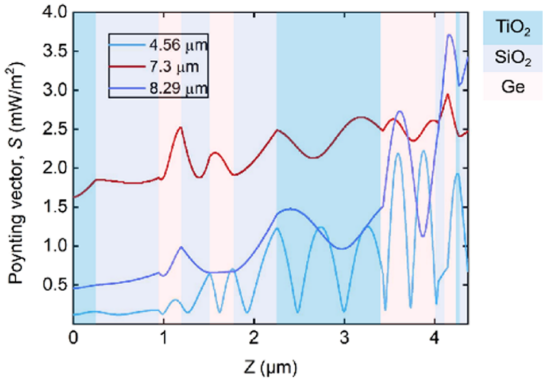

Fig. 4. Poynting vector distribution along the vertical direction, i.e., z axis, of the proposed multilayer film at different wavelengths of 4.56 μm, 7.3 μm, and 8.29 μm. Note that the substrate is attached to the left boundary, and the top surface of the film is on the right.

for radiative property calculation. We define a merit function, which represents the residual error between the emissivity spectrum of a given structure and the target spectrum, and minimizing the merit function is the ultimate goal to achieve. Here we set this function to $F(n, d)$:

$$F(n, d) = \sum_{\lambda} W(\lambda)(\varepsilon(\lambda; n, d) - \varepsilon^*(\lambda))^2, \quad (2)$$

where n is the layer number of the film, d is the thickness of each layer, and $W(\lambda)$ describes the weight for each band. Although the thermal emission at the wavelength band of 0.3–3 μm also needs to be considered at a high temperature, we still want to emphasize the importance of infrared selectivity in the present study. Therefore, here we set the weight of each band as $W(\lambda_{0.3-3\,\mu m}) : W(\lambda_{3-5\,\mu m}) : W(\lambda_{5-8\,\mu m}) : W(\lambda_{8-14\,\mu m}) = 1 : 3 : 3 : 3$. Note that this weight setup should be accordingly redefined referring to specific application conditions, and the optimized outcome will be modified as well. $\varepsilon^*(\lambda)$ is the objective function as shown in Fig. 3(a), and $\varepsilon(\lambda; n, d)$ is spectral emissivity of the multilayer film in the normal direction calculated by the transfer matrix method [30]. At the beginning of the optimization process through the genetic algorithm, a total of 60 cases with SiO_2, TiO_2 and Ge randomly arranged in a 12-layer film are generated as the first generation. The transfer matrix method is employed to calculate the emissivity of the film in the wavelength range between 0.3 μm and 14 μm. The convergence criterion is that the best emissivity curve of each generation does not change within eight generations. After completing the whole optimization process, an optimized multilayer film structure is obtained, and the parameters are listed in Table 1. The calculated spectral emittance associated with this optimized structure is also presented in Fig. 1(c), which demonstrates an excellent performance of selective emission in the infrared range.

To understand the underlying mechanism for the selective infrared emission of the proposed multilayer film structure, we employed the finite difference time domain method [30] to obtain the distribution of radiative energy transport inside each layer of the multilayer film at different wavelengths, by solving the Maxwell equations in three-dimensional space. Figure 4 depicts the Poynting vector spatial distribution in the direction vertical to the film plane at wavelengths of 4.56 μm, 7.3 μm, and 8.29 μm, which correspond to each wavelength range of 3–5 μm, 5–8 μm, and 8–14 μm, respectively. Note that the substrate is attached to the left boundary, and the top surface of the film is on the right. Due to the interference effects, the radiative energy transports like a wave along the vertical direction. For wavelengths of 4.56 μm and 8.29 μm, most of the energy is confined close to the outer surface of the multilayer film, and decreases sharply as it goes to the inside, which indicates high reflection behaving like a metal. However, at the wavelength of 7.3 μm, the Poynting vector could transport much longer inside the film, and there is still a large value transmitted to the substrate, which indicates a large absorption in the substrate. The difference is caused by the constructive or destructive interference effects.

In summary, we have designed a multilayer film with efficient infrared camouflage and thermal management effects along a large temperature range in this study. Combining the genetic algorithm and transfer matrix theory, the material selection and layer thickness are optimized for each layer of the proposed 12-layer film, which demonstrates highly efficient selective infrared emission with a low emissivity in the 3–5 μm and 8–14 μm bands ($\varepsilon_{3\sim5\,\mu m} = 0.14$, $\varepsilon_{8\sim14\,\mu m} = 0.21$) and a high one in the 5–8 μm band ($\varepsilon_{5\sim8\,\mu m} = 0.86$). The selective infrared emission characteristics hardly change over the surface temperature

Table 1. Material Selection and Thickness Setup Assigned for Each Layer of the Proposed Film after Genetic Algorithm Optimization Process

Layer	Substrate	1	2	3	4	5	6	7	8	9	10	11	12
Material	SiO_2	TiO_2	SiO_2	Ge	SiO_2	Ge	SiO_2	TiO_2	Ge	SiO_2	Ge	TiO_2	SiO_2
Thickness (nm)	400 μm	254	694	248	316	271	470	1175	611	104	124	30	71

range from 300 K to 1000 K, and a large range of incidence angles from 0 up to 60 deg. Section S1 of Supplement 1 graphs the emission spectra across that parameter space. As such, the desired functions are maintained. The radiative energy transport distributions inside the proposed film are also plotted at different wavelengths for illustrating the underlying mechanism for selective infrared emission, and the reason for high emission in the spectrum range of 5–8 μm is due to the constructive interference effect. Considering that the materials constructing the proposed film, i.e., SiO_2, TiO_2 and Ge, are all chemically stable and high-temperature endurable, and a total of 12 layers is still among the scope of large-scale fabrication, we believe the proposed film design would find broad applications in areas such as military use for both infrared camouflage and thermal management.

Funding. Science, Technology and Innovation Commission of Shenzhen Municipality (GXWD20201230155427003-20200731100557008); National Natural Science Foundation of China (51806045).

Disclosures. The authors declare no conflicts of interest.

Data Availability. Data underlying the results presented in this Letter are not publicly available at this time but may be obtained from the authors upon reasonable request.

Supplemental document. See Supplement 1 for supporting content.

[†]These authors contributed equally to this Letter.

REFERENCES

1. S. P. Mahulikar, H. R. Sonawane, and G. A. Rao, Prog. Aerosp. Sci. **43**, 218 (2007).
2. N. Baranwal and S. P. Mahulikar, J. Thermophys. Heat Transfer **30**, 854 (2016).
3. P. Long, W. G. Walkup, D. D. Ordinario, E. Karshalev, J.-M. Jocson, A. M. Burke, and A. A. Gorodetsky, Adv. Mater. **25**, 5621 (2013).
4. X. Xie, X. Li, M. Pu, X. Ma, K. Liu, Y. Guo, and X. Luo, Adv. Funct. Mater. **28**, 1706673 (2018).
5. C. Xu, G. T. Stiubianu, and A. A. Gorodetsky, Science **359**, 1495 (2018).
6. L. Xiao, H. Ma, J. Liu, W. Zhao, Y. Jia, Q. Zhao, K. Liu, Y. Wu, Y. Wei, S. Fan, and K. Jiang, Nano Lett. **15**, 8365 (2015).
7. Y. Qu, Q. Li, L. Cai, M. Pan, P. Ghosh, K. Du, and M. Qiu, Light Sci. Appl. **7**, 26 (2018).
8. K.-K. Du, Q. Li, Y.-B. Lyu, J.-C. Ding, Y. Lu, Z.-Y. Cheng, and M. Qiu, Light Sci. Appl. **6**, e16194 (2017).
9. Y. Qu, Q. Li, K. Du, L. Cai, J. Lu, and M. Qiu, Laser Photon. Rev. **11**, 1700091 (2017).
10. M. J. Moghimi, G. Lin, and H. Jiang, Adv. Eng. Mater. **20**, 1800038 (2018).
11. X. Ye, Y. Zhou, Y. Sun, J. Chen, and Z. Wang, Appl. Surf. Sci. **254**, 5975 (2008).
12. Z. Wang, Y. Zhou, and Y. Sun, J. Inorg Organomet. Polym. Mater. **19**, 202 (2008).
13. X. Bu, Y. Zhou, M. He, Z. Chen, and T. Zhang, Appl. Surf. Sci. **288**, 444 (2014).
14. C. Zhang, J. Yang, W. Yuan, J. Zhao, J. Y. Dai, T. C. Guo, J. Liang, G. Y. Xu, Q. Cheng, and T. J. Cui, J. Phys. D **50**, 444002 (2017).
15. C. Zhang, X. Wu, C. Huang, J. Peng, C. Ji, J. Yang, Y. Huang, Y. Guo, and X. Luo, Adv. Mater. Technol. **4**, 1900063 (2019).
16. S. Chandra, D. Franklin, J. Cozart, A. Safaei, and D. Chanda, ACS Photon. **5**, 4513 (2018).
17. O. Salihoglu, H. B. Uzlu, O. Yakar, S. Aas, O. Balci, N. Kakenov, S. Balci, S. Olcum, S. Suzer, and C. Kocabas, Nano Lett. **18**, 4541 (2018).
18. Z. Xu, Q. Li, K. Du, S. Long, Y. Yang, X. Cao, H. Luo, H. Zhu, P. Ghosh, W. Shen, and M. Qiu, Laser Photon. Rev. **14**, 1900162 (2020).
19. B. Liu, J. M. Shi, J. K. Zhang, Z. G. Li, Z. S. Chen, and X. S. Deng, Opt. Mater. **111**, 110689 (2021).
20. H. Zhu, Q. Li, C. Zheng, Y. Hong, Z. Xu, H. Wang, W. Shen, S. Kaur, P. Ghosh, and M. Qiu, Light Sci. Appl. **9**, 60 (2020).
21. H. Zhu, Q. Li, C. Tao, Y. Hong, Z. Xu, W. Shen, S. Kaur, P. Ghosh, and M. Qiu, Nat. Commun. **12**, 1805 (2021).
22. W. Zhang and D. Lv, Opt. Mater. **96**, 110747 (2019).
23. W. Zhang, G. Xu, J. Zhang, H. Wang, and H. Hou, Opt. Mater. **37**, 343 (2014).
24. T. Kim, J.-Y. Bae, N. Lee, and H. H. Cho, Adv. Funct. Mater. **29**, 1807319 (2019).
25. B. Vasić and R. Gajić, Appl. Phys. Lett. **103**, 261111 (2013).
26. L. Peng, D. Liu, H. Cheng, S. Zhou, and M. Zu, Adv. Opt. Mater. **6**, 1801006 (2018).
27. Y. Huang, M. Pu, Z. Zhao, X. Li, X. Ma, and X. Luo, Opt. Commun. **407**, 204 (2018).
28. M. Pan, Y. Huang, Q. Li, H. Luo, H. Zhu, S. Kaur, and M. Qiu, Nano Energy **69**, 104449 (2020).
29. Y. Shi, W. Li, A. Raman, and S. Fan, ACS Photon. **5**, 684 (2017).
30. J. M. Luque-Raigon, J. Halme, and H. Miguez, J. Quant. Spectrosc. Radiat. Transfer **134**, 9 (2014).